# Planarity *vs.* Non-Planarity in the Electronic Communication of TCAQ-Based Push-Pull Chromophores

Raúl García,[a] Joaquín Calbo,[b] Rafael Viruela,[b] Mª Ángeles Herranz,*[a] Enrique Ortí,*[b] and Nazario Martín*[a,c]

Donor-acceptor alkynes, endowed with 11,11,12,12-tetracyano-9,10-anthraquinodimethane (TCAQ) and *N,N*-dimethylaniline (DMA) units, have been further functionalized by a [2+2] tetracyanoethylene (TCNE) cycloaddition followed by a subsequent retroelectrocyclization to form distorted non-planar molecular structures with 1,1,4,4-tetracyanobuta-1,3-diene (TCBD) bridge ligands. Comprehensive spectroscopic, electrochemical, and computational studies have been carried out to compare the electronic communication in these planar (alkyne) and non-planar (with TCBD units) TCAQ-based push-pull chromophores. Cyclic voltammetry and UV-Vis absorption measurements confirm a noticeable electronic communication between the TCAQ and DMA units regardless the quasi-orthogonal arrangement of the two dicyanovinyl halves of the TCBD groups, which partially hinder the electronic communication. The experimental trends are strongly supported by theoretical calculations performed at the density functional theory level, which further evidence an active electron-withdrawing role of the TCBD bridge both in the formation of the charged species and in the lowest-lying absorption features. The novel push-pull TCAQ-based derivatives including the TCBD bridge show a broad absorption in the whole visible range while having a structure highly distorted from planarity. These chromophores may therefore be viewed as appealing candidates to be exploited in photovoltaic devices with minimal aggregation phenomena.

## Introduction

Donor–acceptor (D–A) chromophores, i.e., molecules which present intramolecular charge-transfer processes, represent currently one of the most promising families in the general topics of molecular electronics and optoelectronics.[1] Their intrinsic properties make them ideal for very different applications in fields such as nonlinear optics (NLO),[2] organic light-emitting diodes (OLEDs),[3] organic solar cells,[4] or dye-sensitized solar cells (DSSCs).[5] In contrast to their planar analogues, non-planar D-A chromophores present some differentiating characteristics worthy to study.[6] For example, due to their non-planarity, they have better solubility, which increases drastically their processability and, as a consequence, their applicability. Furthermore, some of them easily sublime and form amorphous films that can be integrated in test devices.[7] Non-planarity also prevents molecular aggregation, which significantly impacts the photophysics and performance of optoelectronic devices.[8]

Despite these properties, it has been only very recently that the π-conjugation relationship between the donor and the acceptor moieties, and the electronic nature of the chromophore, has started to be deeply studied.[9] In general terms, planar systems present a suitable path for electrons that provides a good electronic communication between donor and acceptor units. The rupture of planarity provokes the reduction of the electronic communication, but if this communication is strong enough, non-planar systems will keep exhibiting intramolecular charge transfer, with all the appealing properties associated to this phenomenon.

In the search for new non-planar push-pull systems and the development of new synthetic methodologies, Diederich *et al.* have extensively investigated the formal [2+2] cycloaddition-retroelectrocyclization reaction (CA-RE) between electron-poor alkenes (in many cases tetracyanoethylene, TCNE) and electron-rich alkynes, which yields donor-acceptor substituted buta-1,3-dienes.[10] This methodology has been implemented by many other groups to obtain chromophores with tunable absorptions, which extend into the near-infrared region, and a rich redox chemistry, with quite accessible oxidized and reduced states. However, most of the work in this area has focused on the incorporation of different donors in the alkyne fragment to modulate the efficiency of donor–acceptor conjugation.[11] Only in a few examples it has been reported the presence of both an activating (donor) and a deactivating (acceptor) group connected to the alkyne unit.[12]

In the present study, we have considered an opposite electronic nature of the alkyne substituents, that is, electron-acceptor TCAQ (11,11,12,12-tetracyano-9,10-anthraquinodimethane)[13] and electron-donor *N,N*-dimethylaniline (DMA) units, to build up a series of extended push-pull D−A systems. We have studied the effect that the planarity of the conjugated linker has on the electronic communication between the TCAQ and DMA moieties by comparing the electronic and optical properties of systems bearing a planar alkyne linker with systems incorporating a tetracyanobutadiene (TCBD) unit with a quasi-orthogonal arrangement of its two-dicyanovinyl halves. In this sense, two different TCAQ chromophores were prepared (mono- and di-substituted), with a triple bond connecting the central TCAQ unit and the terminal DMA substituent(s). In this scenario, the two electroactive units (TCAQ and DMA) are planarly connected. However, when this triple bond undergoes a CA-RE reaction

[a] *Dr. R. García, Dr. M. A. Herranz, Prof. Dr. Nazario Martín*
*Departamento de Química Orgánica, Facultad de Química*
*Universidad Complutense de Madrid*
*28040 Madrid (Spain)*
*E-mail: maherran@ucm.es, nazmar@ucm.es*
[b] *Dr. J. Calbo, Dr. P. M. Viruela, Prof. Dr. E. Ortí*
*Instituto de Ciencia Molecular*
*Universidad de Valencia*
*46980 Paterna (Spain)*
*E-mail: enrique.orti@uv.es*
[c] *Prof. Dr. Nazario Martín*
*IMDEA-Nanociencia, c/Faraday 9, Campus Cantoblanco,*
*28049 Madrid (Spain)*

*Supporting information and the ORCID identification number(s) for the author(s) of this article can be found under https://doi.org/101002/cplu.2018XXXXX.*

*Contribution to the Optoelectronics Special Issue*

sequence with TCNE, thus forming two new push-pull chromophores in which one (if TCAQ is mono-substituted) or two (if it is di-substituted) TCBD unit(s) are incorporated, the planar conjugation between TCAQ and DMA is broken, at the time that new acceptor units (TCBD) are added to the structure (Scheme 1). UV-Vis and electrochemical studies, together with density functional theory calculations, have been performed to evaluate the influence that the planarity rupture of the conjugated linker and the incorporation of the TCBD unit(s) has on the redox properties and the intramolecular charge-transfer phenomena observed in these systems.

## Results and Discussion

The synthesis of the new push-pull chromophores **3** and **4** was achieved via a Sonogashira C−C coupling reaction between 2-iodo-11,11,12,12-tetracyano-9,10-anthraquinodimethane (**1**) or 2,6-diiodo-11,11,12,12-tetracyano-9,10-anthraquinodimethane (**2**), which were prepared following a previously reported procedure,[14] and 4-ethynyl-*N,N*-dimethylaniline (Scheme 1). Tetrakis(triphenylphosphine)palladium(0) and copper iodide were employed as catalysts, and triethylamine as base. The procedure yielded the desired products as dark blue solids with good yields (87% for **3**; 71% for **4**). When these products were treated with TCNE in refluxing 1,2-dichloroethane for 12 hours, chromophores **5** and **6** were obtained in 70% and 55% yields, respectively. The introduction of the TCBD units in the structures changed significantly the color of the products from the initial dark blue to dark green. Reaction times up to 5 days produced no increment in the yield of **6**.

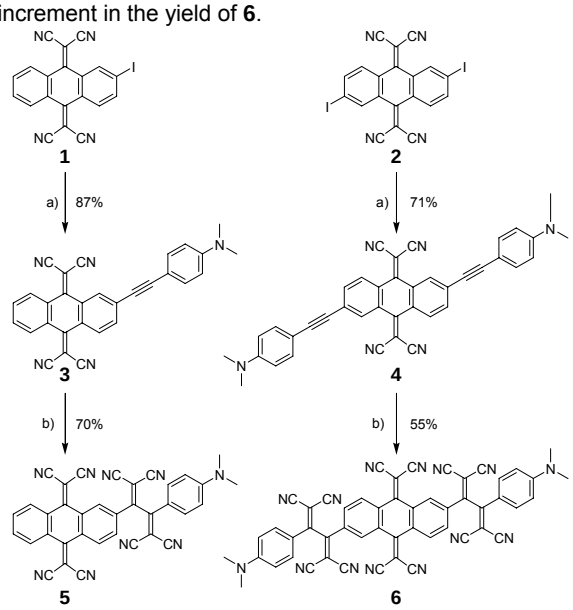


**Scheme 1.** Syntheses of push-pull chromophores **3–6**. Reagents and conditions: a) 4-ethynyl-*N,N*-dimethylaniline, $Pd(PPh_3)_4$, CuI, $NEt_3$, THF; b) TCNE, 1,2-dichloroethane, 80 ºC.

The mechanism of the addition of TCNE to the triple bonds is assumed to be the same as that we reported for π-extended tetrathiafulvalene (exTTF) derivatives.[11e] The addition of one of the π-bonds of the alkyne to one of the electrophilic carbons between the two cyano groups of TCNE produces a high-energy intermediate, which yields a ring-closed product by bond formation of the ionized carbons. Subsequently, the ring-opening cycloreversion gives the product (**5** or **6**), with a quasi-orthogonal disposition of the dicianovinylene units as theoretical calculations demonstrate (see below).

The four new derivatives prepared are colored and stable products, readily soluble in common organic solvents. The structural assignment is based on analytical and spectroscopic techniques (UV-Vis, FTIR, $^1$H and $^{13}$C NMR, and HRMS). For **3** and **4**, the incorporation of the DMA units is noticed with the presence of intense singlets at *ca.* 3.0 ppm in the $^1$H NMR spectra corresponding to the methyl groups. In addition, the *sp* alkyne carbons are easily appreciated in the $^{13}$C NMR spectra between 80 and 100 ppm. In systems **5** and **6**, the multiple cyano substituents provide sharp bands in the FTIR at around 2200 cm$^{-1}$ and in the $^{13}$C NMR at *ca.* 112–116 ppm. For additional details, see the Experimental Section and the Supporting Information (Figures S1–S8).

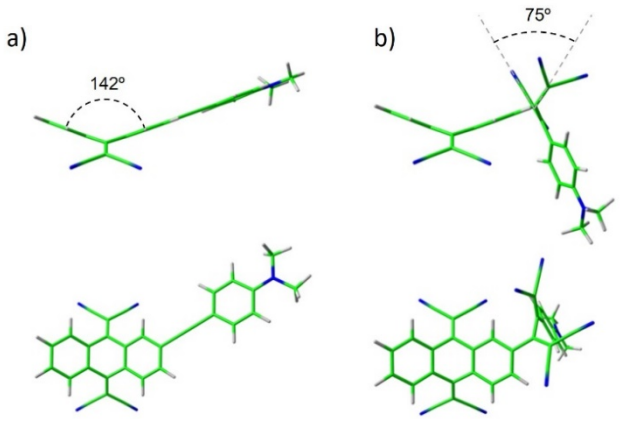


**Figure 1.** Side and top views of the B3LYP/6-31G**-optimized, minimum-energy structure of **3** (a) and **5** (b).

The molecular geometries of the new push-pull chromophores **3–6** were optimized at the B3LYP/6-31G** level in gas phase. Figure 1 displays the minimum-energy structures obtained for the two mono-substituted compounds **3** and **5** (see Figure S9 for di-substituted chromophores **4** and **6**). In all cases, the TCAQ moiety shows its typical butterfly shape with the anthracene unit folded up through the central benzene ring and the dicyanovinylene units pointing in the opposite direction to avoid the steric contacts with hydrogens in *peri*-positions.[15] For **3** (Figure 1a) and **4** (Figure S9), the donor DMA fragment is coplanar to the central anthracene core of TCAQ, which results in an effective conjugation between the TCAQ and the DMA units. The introduction of the TCBD bridge distorts the geometry due to evident steric hindrance, and breaks the π-conjugation between the TCAQ and DMA units in both **5** (Figure 1b) and **6** (Figure S9). The DMA fragment in these orthogonal chromophores is finally oriented downwards, thus resulting in a geometry that clearly resembles that observed for similar exTTF-based derivatives confirmed by X-ray diffraction.[11e]

Electrochemical measurements were carried out to evaluate the impact that the disruption of conjugation, along with the introduction of strong electron-acceptor TCBD units, has on the electronic properties of our push-pull derivatives. The electrochemical characterization of the new compounds **3–6**, and reference TCAQ, TCNE and DMA samples, was carried out

in THF containing 0.1 M $TBAPF_6$ under an argon atmosphere. Figure 2 and Figure S10 display the cyclic voltammograms recorded for **3**–**6**, and Table 1 summarizes the values of the redox potentials obtained.

The first oxidation process of DMA is observed as an irreversible peak at +693 mV for both **3** and **4**, as reported for other arylamine systems.[16] This value is slightly higher than the oxidation potential measured for unsubstituted DMA (+675 mV). Noteworthy, the introduction of the TCBD units induces an important change in the redox properties of compounds **5** and **6**. After a full-oxidative scan, a strong adsorption occurs in the working electrode, and no reductive electrochemistry is later observed. The oxidation of the DMA fragments is indeed found much more difficult for **5** and **6** –near the solvent window limit– than in **3** and **4** (Table 1), due to the direct connection to the strong TCBD acceptor.

The reduction of the TCAQ derivatives **3** and **4** occurs in a single, unresolved, reversible, two-electron step, similarly to that observed for the parent TCAQ (Figure 2).[17] The peak-to-peak potential difference ranges from 90 to 130 mV, and addition of the DMA unit(s) to the TCAQ core results in a small decrease of the first reduction potentials compared to that of unsubstituted TCAQ (Table 1). This seems to be more an effect of chain lengthening than due to the electronic communication with a not particularly powerful DMA electron donor.

**Table 1.** Cyclic voltammetry redox potentials (in mV) for **3**–**6** and reference compounds (THF, 0.1 M $TBAPF_6$).[a]

| | $E^{pa}_{ox,1}$[b] | $E^{pa}_{ox,2}$[b] | $E^{1/2}_{red,1}$ | $E^{1/2}_{red,2}$ | $E^{1/2}_{red,3}$ |
|---|---|---|---|---|---|
| **TCAQ** | – | – | –665 | – | – |
| **TCNE** | – | – | –24 | –1112 | – |
| **DMA** | +675 | – | – | – | – |
| **3** | +693 | +854 | –616 | – | – |
| **4** | +693 | +858 | –596 | – | – |
| **5** | +1084 | – | –532 | –899 | –1220 |
| **6** | +1046 | – | –451 | –820 | –1148 |

[a] Potentials versus $Ag/AgNO_3$. Working electrode: glassy carbon electrode; counter electrode: Pt; reference electrode: $Ag/AgNO_3$. Scan rate: 0.1 $V \cdot s^{-1}$. $E^{1/2} = (E^{pa} + E^{pc})/2$, where $E^{pc}$ and $E^{pa}$ = cathodic and anodic peak potentials, respectively. [b] Anodic peak potential.

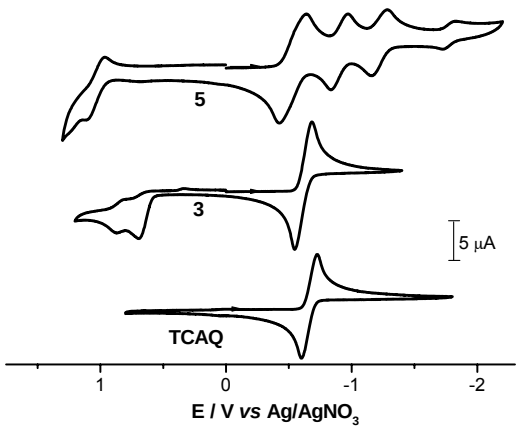


**Figure 2.** Cyclic voltammograms of TCAQ and compounds **3** and **5** in THF, 0.1 M $TBAPF_6$, recorded at a scan rate of 100 $mV \cdot s^{-1}$.

Compound **5** presents three reversible reduction waves at –532, –899, and –1220 mV (Figure 2). The first reduction seems to be a two-electron process, most probably corresponding to the TCAQ core, as it is indicated by the peak current intensities. The extension of the conjugation with electron-acceptor TCBD groups makes this reduction easier (compare $E^{1/2}_{red,1}$ values for **3** and **5** in Table 1). The second and third reduction waves involve one electron each, and correspond to the reduction of the dicyanovinylene units of the TCBD moiety. The cyclic voltammogram of **6** is much broader (Figure S10), which makes more difficult the assignment of the different processes. However, similar observations to those mentioned for **5** can be deduced by the deconvolution of the CV (Figure S10).

Theoretical calculations further corroborate the electronic properties observed for chromophores **3**–**6,** and shed light into the communication between their electronically active, constituting moieties. Figure 3 displays the atomic orbital composition of the highest-occupied (HOMO) and lowest-unoccupied molecular orbital (LUMO) for **3** and **5** (see Figure S11 for an extended list of frontier molecular orbitals). The HOMO is mainly localized on the electron-donor dimethylaniline (DMA) fragment for both derivatives. In **3**, the HOMO spreads over the TCAQ moiety evidencing the electronic connection between the two molecular fragments that are efficiently conjugated through the alkyne linker because of their coplanar disposition (Figure 1a). In **5**, this π-conjugation is broken due to the quasi-orthogonal disposition of the donor and acceptor groups promoted by the TCBD bridge (Figure 1b), and the TCAQ no longer contributes to the HOMO. Otherwise, the LUMO and LUMO+1 are completely localized on the acceptor TCAQ moiety in **3** (Figure 3). The LUMO of **5** also lies on the TCAQ moiety as for **3**, but now the LUMO+1 involves both the TCAQ moiety and the electron-accepting TCBD group (Figure 3).

The description of the molecular orbitals for mono-substituted **3** and **5** can be applied to the di-substituted **4** and **6** analogues, respectively (Figure S12). Two practically degenerated HOMOs are predicted for **4** and **6** due to the double substitution of TCAQ with DMA units. The degeneracy in **4** is less marked than in **6** because of the existence of a small coupling between the two donor fragments in the former (Figure 4 and Table S1). This coupling is provoked by the high electron delocalization through the π-conjugated linkers (Figure S12).

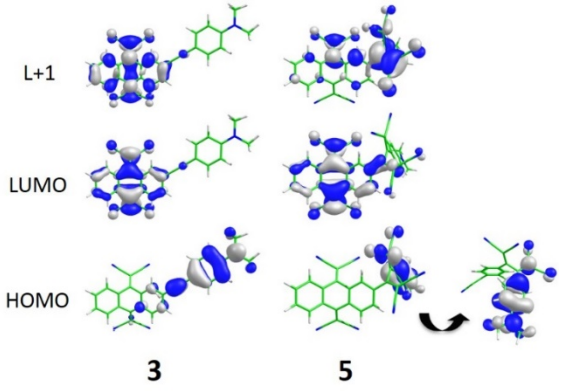


**Figure 3.** Isovalue contours (±0.03 a.u.) calculated for the HOMOs and LUMOs of **3** and **5** at the B3LYP/6-31G** level. Two different views are included for the HOMO of **5** to illustrate the localization of the MO and the lack of conjugation with the TCAQ moiety.

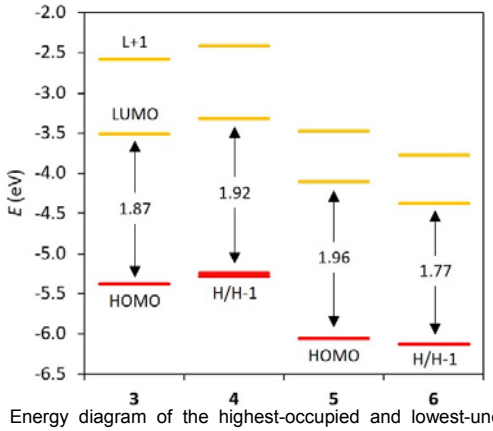


**Figure 4.** Energy diagram of the highest-occupied and lowest-unoccupied molecular orbitals for the push-pull TCAQ derivatives **3**–**6**. H and L denote HOMO and LUMO, respectively.

Theoretical calculations predict a significant stabilization of the HOMO in going from the planar derivatives **3** (–5.39 eV) and **4** (–5.25 eV) to the orthogonal systems **5** (–6.06 eV) and **6** (–6.14 eV). These trends are in line with the shift to higher potentials of the first oxidation wave recorded experimentally for **5** and **6** compared with **3** and **4** (Table 1), and with the ionization potentials calculated for **5** (7.36 eV) and **6** (7.03 eV) that are significantly higher than those obtained for **3** (6.61 eV) and **4** (6.12 eV) (Table S2). Spin densities (Figure 5 for **5** and Figure S13 for the rest of derivatives) and accumulated Mulliken charges (Table S3) confirm that upon oxidation the charge is mainly extracted from the electron-rich DMA.

Similarly to the HOMO energy trends, the TCAQ-centered LUMO of **3** (–3.51 eV) and **4** (–3.32 eV) is significantly stabilized moving to the orthogonal **5** (–4.10 eV) and **6** (–4.37 eV) derivatives due to the strong electron-withdrawing character of the TCBD units to which TCAQ is attached. Spin densities (Figure 5 for **5** and Figure S14 for the rest of derivatives) and accumulated charges (Table S4) calculated for the anion species confirm that the reduction process takes place on the TCAQ moiety for the first and second electron insertions. Interestingly, the anthracene core of the TCAQ moiety planarizes upon formation of the dianion species, and the dicyanovinylene groups tilt out the anthracene plane by 45º (Figure S15). The global electron affinity (EA) for the two-electron reduction process is calculated to be 1.96, 2.02, 3.30, and 4.38 eV for **3**–**6**, respectively, evidencing a larger facility to reduce the TCBD-containing derivatives **5** and **6**. These results are in full accord with the $E^{1/2}_{red,1}$ values measured experimentally (Table 1).

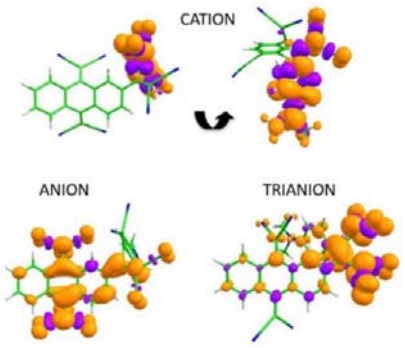


**Figure 5**. Spin density contours (±0.001 a.u.) calculated for the cation, anion, and trianion species of **5** at the B3LYP/6-31G** level of theory. Two different views are included for the cation.

The reduction process involving the insertion of a third electron is demonstrated to be highly unfavorable for the planar chromophores **3** and **4**, with theoretical EA values of –3.93 and –3.37 eV, respectively. This result agrees with the absence of any negative-potential wave in the electrochemical experiments after the reduction of the TCAQ unit (Figure 2 for **3** and Figure S10 for **4**). Conversely, this process is affordable experimentally for **5** and **6**, for which lower EA values of –1.97 and –0.99 eV are calculated, respectively. The electron-withdrawing TCBD moieties of **5** and **6** have a primary role in stabilizing the introduction of the third electron (Figure 5 and Figure S16), with an accumulated negative charge of more than 1.0e on each unit (Table S4).

The optical properties of chromophores **3**–**6** were also investigated by solution UV-Vis spectroscopy and quantum-chemistry calculations.

The UV-Vis spectra of all compounds were registered in five different solvents: toluene, tetrahydrofuran, dichloromethane, acetonitrile and methanol. All derivatives feature strong absorptions between 250 and 400 nm, as expected for these systems containing the TCAQ unit (Figure 6 and Figure S17). In addition, compounds **3** and **4** present a strong band centered at a $\lambda_{max}$ between 507 and 558 (see Table 2 for specific data), which is highly sensitive to solvent polarity. With the exception of dichloromethane, both derivatives exhibit a hypsochromic shift of this band upon increasing solvent polarity. This behavior could correspond to an intramolecular charge transfer (CT) from the peripheral DMA donor group(s) into the TCAQ core. Typically, a polar D-π-A system is more stabilized in the excited state than in the less-polar ground state in solvents with a large dielectric constant, and this should result in a bathochromic shift of the CT band. However, other effects, such a permanent dipole moment or molar volume cannot be ruled out.[18] For the non-planar chromophores **5** (Figure 6) and **6** (Figure S17), the longest-wavelength absorption maximum shifts hypsochromically to 467–480 nm, and remains mostly unaffected to changes in solvent polarity. In addition to this strong band, there is a second, very weak transition around 526–605 nm, leading to the tailing on the end-absorption around 730–800 nm. The presence of this presumably CT band indicates a significant electronic communication between the donor and acceptor fragments, despite the non-planarity of molecules **5** and **6**.

Vertical electronic transition energies were computed for chromophores **3**–**6** at the MPWB1K/6-31G** level using the time-dependent density functional theory (TD-DFT) approach and including solvent effects (see the Experimental Section). Table 3 summarizes the energies and electronic nature calculated, in dichloromethane, for the most relevant singlet excited states ($S_n$) involved in the experimental UV-Vis spectra of **3** and **5**. The electronic description of the absorption spectra recorded for the di-substituted chromophores **4** and **6** (see Table S6) is similar to that described below for the mono-substituted analogues (see also Figure S18 for the theoretical simulation of the absorption spectra for **3**–**6**).

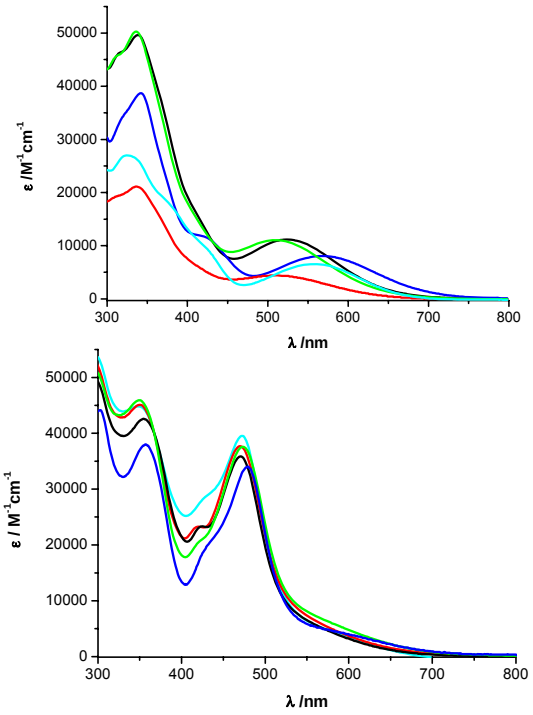


**Figure 6.** UV-Vis spectra of compounds **3** (top) and **5** (bottom) measured in several solvents: toluene (cyan), tetrahydrofuran (black), dichloromethane (blue), acetonitrile (green), and methanol (red).

**Table 2.** Longest-wavelength absorption maxima $\lambda_{max}$ of the CT bands measured for **3**-**6** in different solvents.

| | | Wavelenght, $\lambda_{max}$ (nm) | | | |
|---|---|---|---|---|---|
| Solvent | $E_T^N$ [a] | **3** | **4** | **5**[b] | **6**[b] |
| Toluene | 0.099 | 558 | 555 | 473 (602) | 467 (526) |
| Tetrahydrofuran | 0.207 | 524 | 523 | 471 (604) | 466 (560) |
| Dichloromethane | 0.309 | 568 | 555 | 480 (625) | 480 (600) |
| Acetonitrile | 0.460 | 509 | 507 | 473 (604) | 470 (556) |
| Methanol | 0.762 | 509 | 507 | 469 (605) | 473 (550) |

[a] Normalized solvent polarity parameter ($E_T^N$): C. Reichardt, *Solvents and Solvent Effects in Organic Chemistry*. Wiley-VCH, Weinheim, 2004. [b] Values in brackets correspond to probably a second, very weak CT transition for compounds **5** and **6**.

**Table 3.** Lowest singlet excited states calculated for **3** and **5** at the TD-MPWB1K/6-31G** level in dichloromethane. Vertical excitation energies (*E*), oscillator strengths (*f*), dominant monoexcitations with contributions (within parenthesis) greater than 35%, and description of the excited states are given. H and L denote HOMO and LUMO, respectively.

| State | *E* (eV) | *E* (nm) | *f* | Monoexcitation (%) | Description |
|---|---|---|---|---|---|
| **Compound 3** | | | | | |
| $S_1$ | 2.174 | 570 | 0.4416 | H → L (95) | DMA → TCAQ |
| $S_2$ | 3.123 | 397 | 0.6331 | H → L+1 (90) | DMA → TCAQ |
| $S_4$ | 3.561 | 348 | 0.4692 | H-2 → L (79) | TCAQ |
| **Compound 5** | | | | | |
| $S_1$ | 2.341 | 530 | 0.0161 | H → L (82) | DMA → TCAQ |
| $S_2$ | 2.731 | 454 | 0.1902 | H → L+1 (81) | DMA → TCBD |
| $S_3$ | 3.243 | 382 | 0.5269 | H → L+2 (81) | DMA → TCAQ/TCBD |
| $S_4$ | 3.480 | 356 | 0.4550 | H-1 → L (77) | TCAQ |
| $S_5$ | 3.601 | 344 | 0.3679 | H-4 → L (39) | TCAQ |

The first low-energy band observed in the experimental UV-Vis spectrum for **3** at 500–600 nm (Figure 6) corresponds to the electronic transition to the lowest-lying singlet excited state $S_1$, calculated at 570 nm with an oscillator strength (*f*) of 0.442, which results from the HOMO→LUMO one-electron promotion (Table 3). The hypsochromic shift experimentally recorded upon increasing solvent polarity for this band is however barely captured by the continuum solvent model (Table S5). Otherwise, the shoulder recorded around 400 nm for **3** originates from the HOMO→LUMO+1 monoexcitation, and corresponds to the transition to the $S_2$ state calculated at 397 nm. These two electronic transitions imply an intramolecular charge transfer from the DMA donor unit, where the HOMO is located, to the TCAQ acceptor moiety, where the LUMO and LUMO+1 reside (Figure 3). The $S_0 \rightarrow S_1$ and $S_0 \rightarrow S_2$ transitions have a remarkable intensity due to the overlap between the molecular orbitals involved (HOMO and LUMO/LUMO+1), in line with the efficient electronic conjugation between the acceptor and the donor fragments. Finally, the intense band observed for **3** around 300–350 nm is assigned to several local $\pi \rightarrow \pi^*$ transitions computed in this range (Figure S18), which mainly involve the electron-accepting TCAQ core (e.g., the $S_0 \rightarrow S_4$ transition calculated at 348 nm with a $f = 0.469$, Table 3). States $S_1$, $S_2$ and $S_4$ therefore lead to an intense optical absorption for **3** covering the whole visible range.

The absorption spectrum recorded for the TCBD-containing analogue **5** significantly differs from that of planar **3**. Theoretical calculations predict for orthogonal **5** a very weak transition $S_0 \rightarrow S_1$ at 530 nm with a $f = 0.016$ that corresponds to the tail observed in the UV-Vis spectrum around 550 nm (Figure 6). The nature of this transition is mainly determined by the charge-transfer HOMO→LUMO monoexcitation from the DMA moiety to the acceptor TCAQ fragment (Table 3). The weakness of the $S_0 \rightarrow S_1$ intensity is attributed to the TCBD linkage that produces a break in the conjugation –orthogonal disposition of the donor and acceptor moieties– and a reduction of the overlap between the HOMO and LUMO involved in the transition (Figure 3). The transition to the second singlet excited state $S_2$ is calculated at 454 nm with an oscillator strength of 0.190, and gives rise to the band experimentally recorded at 450–500 nm. The $S_0 \rightarrow S_2$ transition is assigned predominantly to the HOMO→LUMO+1 monoexcitation, and is described as an intramolecular CT excitation from the donor DMA to the acceptor TCBD unit (Table 3). In fact, this characteristic transition is observed in a plenty of DMA derivatives where dicyanovinyl groups are introduced as acceptor fragments.[18c,19] Finally, the intense absorption band recorded experimentally around 350 nm in chromophore **5** is attributed to transitions to states $S_4$ and $S_5$ calculated at 356 and 344 nm with $f = 0.455$ and 0.368, respectively. These states imply local excitations centered in the electron-acceptor TCAQ moiety, in analogy to that predicted for **3**. Additionally, a charge-transfer $S_3$ state described by one-electron promotion from DMA to TCAQ/TCBD is calculated at 382 nm with a significant oscillator strength of $f = 0.527$ (Table 3). This $S_0 \rightarrow S_3$ CT transition also contributes to the experimental band centered at 350 nm. In spite of the conjugation breaking promoted by the orthogonal TCBD bridge, the donor DMA and the acceptor TCBD and TCAQ units in **5** are therefore electronically communicated, and lead to intense CT transitions allowing a large absorption in the whole range of the visible spectrum.

## Conclusions

By using a formal [2+2] cycloaddition-retroelectrocyclization (CA-RE) reaction, TCBD units have been introduced on the triple bonds that connect one or two DMA donor units to a TCAQ acceptor. We have thoroughly studied and compared the electronic communication in these planar and non-planar TCAQ-based push-pull chromophores, establishing the importance that planarity has in charge-transfer processes. By means of this study, it can be assessed that planarity facilitates conjugation, but in non-planar chromophores with an adequate design, a significant electronic communication remains. These statements have been experimentally supported by UV-Vis and electrochemical measurements, as well as by theoretical calculations carried out by using the DFT approach. Importantly, our chromophores absorb light in the whole visible range of the spectrum with intense charge-transfer excitations, even in the orthogonally-disposed TCBD-containing derivatives. We therefore present an interesting strategy for obtaining push-pull chromophores as potential candidates to be exploited in a wide range of applications in the field of electronics and photovoltaics.

## Experimental Section

### Materials and General Methods

All solvents were dried according to standard procedures. Reagents were used as purchased. 2-iodo-11,11,12,12-tetracyano-9,10-anthraquinodimethane (**1**) or 2,6-diiodo-11,11,12,12-tetracyano-9,10-anthraquinodimethane (**2**) were prepared using the previously described procedures.[13,14] All air-sensitive reactions were carried out under argon atmosphere. Flash chromatography was performed using silica gel (230–240 mesh). Analytical thin layer chromatography (TLC) was performed using aluminium-coated plates. Melting points were determined on a Gallenkamp apparatus and are uncorrected. NMR spectra were recorded on Bruker Avance 300 spectrometer at 298 K using partially deuterated solvents as internal standards. Coupling constants (*J*) are denoted in Hz and chemical shifts ($\delta$) in ppm. Multiplicities are denoted as follows: s = singlet, d = doublet, t = triplet, m = multiplet, br = broad. FT-IR spectra were recorded on a Bruker Tensor 27 (ATR device) spectrometer. UV-Vis spectra were recorded on a Varian Cary 50 spectrophotometer. Electrospray Ionization Mass Spectra (ESI-MS) and Matrix Assisted Laser Desorption Ionization (coupled to a Time-Of-Flight analyzer) experiments (MALDI-TOF) were recorded on a HP1100MSD spectrometer and a Bruker REFLEX spectrometer, respectively.

### Electrochemistry

Electrochemical measurements were performed at room temperature in a potentiostate/galvanostate Autolab PGSTAT30. Measurements were carried out in a home-built one-compartment cell with a three-electrode configuration, containing 0.1 M tetrabutylammonium hexafluorophosphate ($TBAPF_6$) as supporting electrolyte. A glassy carbon (GCE) was used as the working electrode, a platinum wire as the counter electrode, and a $Ag/AgNO_3$ non-aqueous electrode was used as reference. Prior to each voltammetric measurement the cell was degassed under an argon atmosphere by *ca.* 20 min. The solvent, THF, was freshly distilled from Na. The electrochemical measurements were performed using a concentration of approximately 0.2 mM of the corresponding compound.

### Theoretical Calculations

Quantum-chemical calculations were performed under the density functional theory (DFT) framework by means of the Gaussian 09.D01 suite of programs.[20] Minimum-energy structures were obtained using the popular hybrid exchange-correlation Becke3-Lee-Yan-Parr B3LYP functional[21] and the split-valence double-ζ Pople's 6-31G** basis set.[22] Singly-charged cations and anions and triply-charged trianions were optimized as open-shell species using the unrestricted UB3LYP/6-31G** approach. Doubly-charged dications and dianions were calculated as closed-shell systems. Ionization potential (IP) and electron affinity (EA) values associated to the different oxidation and reduction processes, respectively, were calculated under the adiabatic approximation. Molecular orbital and spin density isovalue contours were represented with the Chemcraft 1.8 software.[23]

Lowest-lying singlet excited states were computed under the time-dependent density functional theory[24] in solution. The popular global-hybrid meta-GGA MPWB1K functional of Truhlar et al.[25] was employed along with the 6-31G** basis set. Solvent effects were captured by employing the self-consistent reaction field (SCRF) method and the polarizable continuum model (PCM)[26] with dichloromethane as solvent. A list of solvents with different dielectric constants were used to analyse the solvatochromism of the lowest-lying absorption bands in derivative **3**.

**2-[(4-Dimethylaminophenyl)ethynyl]-9,10-bis(dicyanomethylen)-9,10-dihydroanthracene (3):** To a solution of 2-iodo-11,11,12,12-tetracyano-9,10-anthraquinodimethane **1** (200 mg, 0.47 mmol) in dry THF (30 mL) under argon atmosphere, $Pd(PPh_3)_4$ (28 mg, 0.024 mmol), CuI (5 mg, 0.024 mmol), and subsequently 4-ethynyl-*N,N*-dimethylaniline (88 mg, 0.47 mmol) and triethylamine (0.3 mL) were added. The mixture was allowed to stir overnight, and then was washed with $NH_4Cl$, $H_2O$, and brine. Afterwards, the solvent was evaporated and the crude product purified by silica gel flash column chromatography (silica gel, hexane:dichloromethane 1:1) to afford **3** as a dark blue solid (87% yield). M.p. > 300 ºC; $^1$H NMR ($CDCl_3$, 300 MHz): $\delta$ = 8.24 (m, 4H), 7.75 (m, 3H), 7.46 (d, 2H), 7.46 (m, 2H, *J* = 8.9 Hz), 6.68 (m, 2H, *J* = 8.9 Hz), 3.03 (s, 6H) ppm; $^{13}$C NMR ($CDCl_3$, 75 MHz): $\delta$ = 158.9, 158.5, 149.9, 149.6, 136.8, 133.2, 132.5, 131.5, 131.4, 131.4, 129.5, 129.3, 129.1, 129.0, 128.7, 128.4, 126.7, 126.6, 126.5, 112.3, 112.2, 112.0, 111.8, 110.7, 107.0, 97.6, 85.4, 82.4, 81.2, 39.1 ppm; FTIR (KBr): $\nu$ = 2921, 2857, 2198, 1591, 1555, 1524, 1446, 1367, 1336, 1272, 1179, 1140, 1109, 1068, 816, 759, 734, 691, 64 $cm^{-1}$; UV/Vis ($CH_2Cl_2$): $\lambda_{max}$ ($\varepsilon$) = 345 (38019), 422 (11749), 569 (7943) nm ($M^{-1}$ $cm^{-1}$); HRMS (ESI): calcd. for $[C_{30}H_{17}N_5]^+$ 447.14882; found 447.14894.

**2,6-Bis[(4-dimethylaminophenyl)ethynyl]-9,10-bis(dicyanomethylen)-9,10-dihydroanthracene (4):** To a solution of 2,6-diiodo-11,11,12,12-tetracyano-9,10-anthraquinodimethane **2** (100 mg, 0.18 mmol) in dry THF (30 mL) under argon atmosphere, $Pd(PPh_3)_4$ (21 mg, 0.022 mmol), CuI (4 mg, 0.022 mmol), and subsequently 4-ethynyl-*N,N*-dimethylaniline (52 mg, 0.36 mmol) and triethylamine (0.1 mL) were added. The mixture was allowed to stir overnight, and then was washed with $NH_4Cl$, $H_2O$, and brine. Afterwards, the solvent was evaporated and the crude product purified by silica gel flash column chromatography (silica gel, dichloromethane) to afford compound **4** as a dark blue solid (71% yield). M.p. > 300 ºC; $^1$H NMR ($CDCl_3$, 300 MHz): $\delta$ = 8.26 (d, 2H, *J* = 1.30 Hz), 8.17 (d, 2H, *J* = 8.10 Hz), 7.75 (m, 2H), 7.45 (d, 3H, *J* = 8.90 Hz), 7.38 (d, 1H, *J* = 8.80 Hz), 6.68 (d, 3H, *J* = 8.90 Hz), 6.63 (d, 1H, *J* = 8.90 Hz), 3.04 (s, 9H), 2.99 (s, 3H) ppm; $^{13}$C NMR (THF-$d_8$, 75 MHz): $\delta$ = 158.9, 158.5, 149.9, 133.2, 133.1, 132.5, 132.2, 131.5, 131.4, 129.6, 129.5, 129.3, 129.2, 129.1, 128.7, 128.3, 128.3, 126.7, 126.6, 126.6, 112.3, 112.2, 112.0, 111.8, 110.7, 107.1, 107.0, 97.5, 97.5, 85.4, 85.4, 82.4, 81.4, 81.2, 39.1, 39.1 ppm; FTIR (KBr): $\nu$ = 2918, 2197, 1593, 1552, 1525, 1478, 1445, 1366, 1332, 1268, 1228, 1177, 1141, 1107, 1061, 945, 904, 815, 766, 699, 635 $cm^{-1}$; UV/Vis ($CH_2Cl_2$): $\lambda_{max}$ ($\varepsilon$) = 342 (18197), 421 (7943), 560 (3090) nm ($M^{-1}$ $cm^{-1}$); HRMS (MALDI-TOF): calcd. for $[C_{40}H_{26}N_6]^+$ 590.021; found 590.020.

**2-[3-(4-dimethylaminophenyl)-1,1,4,4-tetracyano-1,3-butadien-2-yl]-9,10-bis(dicyanomethylen)-9,10-dihydroanthracene (5):** A mixture of **3** (50 mg, 0.11 mmol.) and TCNE (42 mg, 0.33 mmol) dissolved in 1,2 dichloroethane (15 mL) was refluxed overnight under argon atmosphere. After that, the solvent was evaporated and the crude was purified by

column chromatography on silica gel using dichloromethane as eluent to afford **3** as a dark green solid (70 % yield). M.p. > 300 ºC; $^1$H NMR ($CDCl_3$, 300 MHz): $\delta$ = 8.45 (d, 1H, $J$ = 8.40 Hz), 8.28 (m, 3H), 8.20 (m, 1H), 7.82 (m, 4H), 6.79 (d, 1H, $J$ = 9.30 Hz), 3.23 (s, 6H) ppm; $^{13}$C NMR ($CDCl_3$, 75 MHz): $\delta$ = 173.1, 162.1, 155.5, 134.3, 133.6, 133.3, 133.2, 131.8, 130.3, 130.1, 128.4, 124.2, 122.3, 122.1, 114.4, 113.3, 81.1, 61.4, 40.9, 39.4 ppm; FTIR (KBr): $\nu$ = 2925, 2856, 2216, 1737, 1606, 1564, 1491, 1386, 1350, 1262, 1213, 1178, 1094, 1024, 945, 802, 754, 715, 653 cm$^{-1}$; UV/Vis ($CH_2Cl_2$): $\lambda_{max}$ ($\varepsilon$) = 357 (38019), 437 (20417), 479 (33113), 582 (4786) nm (M$^{-1}$ cm$^{-1}$); HRMS (ESI): calcd. for $[C_{36}H_{17}N_9]^+$ 575.16070; found 575.16124.

**2,6-Bis[3-(4-dimethylaminophenyl)-1,1,4,4-tetracyano-1,3-butadien-2-yl]-9,10-bis(dicyanomethylen)-9,10-dihydroanthracene (6):** To a solution of 40 mg (0.07 mmol) of **5** in 1,2-dichloroethane (15 mL) heated to 80 ºC, were added 52 mg (0.41 mmol) of TCNE under argon atmosphere. The mixture was allowed to stir overnight, and then the solvent was evaporated under reduced pressure and the crude was purified by column chromatography using dichloromethane as eluent, to afford **6** as a dark green solid (55% yield). M.p. > 300 ºC; $^1$H NMR ($CDCl_3$, 300 MHz): $\delta$ = 8.58 (d, 2H, $J$ = 1.60 Hz), 8.42 (d, 2H, $J$ = 8.40 Hz), 8.15 (dd, 2H, $J_1$ = 8.40 Hz, $J_2$ = 1.60 Hz), 7.80 (d, 4H, $J$ = 9.40 Hz), 6.78 (d, 4H, $J$ = 9.40 Hz), 3.22 (s, 12H) ppm; $^{13}$C NMR ($CDCl_3$, 75 MHz): $\delta$ = 176.6, 176.1, 158.0, 155.7, 135.1, 134.9, 133.1, 132.7, 132.4, 131.7, 131.5, 129.0, 116.8, 115.6, 113.4, 112.2, 58.3, 57.0, 40.8 ppm; FTIR (KBr): $\nu$ = 2924, 2857, 2219, 1735, 1605, 1489, 1385, 1348, 1264, 1216, 1179, 1080, 1031, 771, 686, 622 cm$^{-1}$; UV/Vis ($CH_2Cl_2$): $\lambda_{max}$ ($\varepsilon$) = 354 (27542), 442 (14791), 479 (23442), 575 (3236) nm (M$^{-1}$ cm$^{-1}$); HRMS (MALDI-TOF): calcd. for $[C_{52}H_{26}N_{14}]^+$ 846.910; found 846.909.

## Acknowledgements

*Financial support from the European Research Council (ERC-320441-Chirallcarbon), MINECO of Spain (CTQ2014-52045-R, CTQ2015-71154-P, CTQ2016-81911-REDT and Unidad de Excelencia María de Maeztu MDM-2015-0538), Comunidad de Madrid (S2013/MIT-2841) Generalitat Valenciana (PROMETEO/2016/135), and european Feder funds (CTQ2015-71154-P) is acknowledged. J.C. is thankful to the Generalitat Valenciana for a postdoctoral fellowship (APOSTD/2017/081).*

## Conflict of interest

*The authors declare no conflict of interest.*

**Keywords:** donor-acceptor systems • cycloaddition/electrocyclization reactions • tetracyanobutadiene• non-planar linkers• density functional calculations

[1] Special issues and reviews devoted to Organic Electronics and Optoelectronics: a) U. Scherf, H. Tian, *Adv. Mater.* **2012**, *24* (issue 5), 569-703; b) S. R. Forrest, M. E. Thompson, *Chem. Rev.* **2007**, *107* (issue 4), 923-1386; c) D. M. Guldi, B. M. Illescas, C. M. Atienza, M. Wielopolski, N. Martín, *Chem. Soc. Rev.* **2009**, *38*, 1587-1597.

[2] a) E. Cariati, X. Liu, Y. Geng, A. Forni, E. Lucenti, S. Righetto, S. Decurtins, S.-X. Liu, *Phys. Chem. Chem. Phys*. **2017**,*19*, 22573-22579; b) A. B. Marco, N. Martínez de Baroja, S. Franco, J. Garín, J. Orduna, B. Villacampa, A. Revuelto, R. Andreu, *Chem. Asian J.* **2015***, 10,* 188-197; c) L. R. Dalton, P. A. Sullivan, D. H. Bale, *Chem. Rev.* **2010**, *110*, 25-55.

[3] a) L. Yao, S. Zhang, R. Wang, W. Li, F. Shen, B. Yang, Y. Ma, *Angew. Chem. Int. Ed.* **2014**, *53*, 2119-2123; b) W. Brütting, J. Frischeisen, T. D. Schmidt, B. J. Scholz, C. Mayr, *Phys. Status Solidi A* **2013**, *210*, 44-65.

[4] a) N. Martín, *Adv. Energy Mat.* **2017**, *7*, 1601102; b) R. Sandoval-Torrientes, J. Calbo, W. Matsuda, W. Choi, J. Santos, S. Seki, E. Ortí, N. Martín, *ChemPlusChem* **2017**, *82*, 1105-1111; c) L. Hammarström, *Acc. Chem. Res.* **2015**, *48* ,840–850; d) K. A. Mazzio, C. K. Luscombe, *Chem. Soc. Rev.* **2015**, *44*, 78-90; e) T. Ameri, N. Lia, C. J. Brabec, *Energy Environ. Sci.* **2013**,*6*, 2390-2413.

[5] a) M. Wielopolski, M. Marszalek, F. G. Brunetti, D Joly, J. Calbo, J. Aragó, J.-E. Moser, R. Humphry-Baker, S. M. Zakeeruddin, J. L. Delgado, M. Gratzel, E. Ortí, N. Martín, *J. Mater. Chem. C* **2016**, *4*, 3798-3808; b) Z. Yao, M. Zhang, H. Wu, L. Yang, R. Li, P. Wang, J. *Am. Chem. Soc.* **2015**, *137*, 3799-3802; c) Z. Yu, F. Li, L. Sun, *Energy Environ. Sci.* **2015**, *8*, 760-775; d) J. Calbo, M. Pastore, E. Mosconi, E. Ortí, F. De Angelis, *Phys. Chem. Chem. Phys.* **2014**, *16*, 4709-4719; e) P.-A. Bouit, L. Infantes, J. Calbo, R. Viruela, E. Ortí, J. L. Delgado, N. Martín, *Org. Lett.* **2013**, *15*, 4166-4169; f) P.-A. Bouit, M. Marszalek, R. Humphry-Baker, R. Viruela, E. Ortí, S. M. Zakeeruddin, M. Grätzel, J. L. Delgado, N. Martín, *Chem. Eur. J.* **2012**, *18*, 11621-11629; g) B. E. Hardin, H. J. Snaith, M. D. McGehee, *Nature Photonics* **2012**, *6*, 162-169.

[6] a) K. Nagarajan, A. R. Mallia, K. Muraleedharan, M. Hariharan*, Chem. Sci.* **2017**, *8*, 1776-1782; b) T. M. Pappenfus, D. K. Schneiderman, J. Casado, J. T. López Navarrete, M. C. Ruiz Delgado, G. Zotti, B. Vercelli, M. D. Lovander, L. M. Hinkle, J. N. Bohnsack, K. R. Mann, *Chem. Mater.* **2011**, *23*, 823-831.

[7] a) I. S. Park, H. Komiyama, T. Yasuda, *Chem. Sci.* **2017**, *8*, 953-960; b) H. Tsujimoto, D.-G. Ha, G. Markopoulos, H. S. Chae, M. A. Baldo, T. M. Swager, *J. Am. Chem. Soc.* **2017**, *139*, 4894-4900.

[8] a) C. H. Y. Ho, H. Cao, Y. Lu, T.-K. Lau, S. H. Cheung. H.-W. Li, H. Yin, K. L. Chiu, L.-K. Ma, Y. Cheng, S.-W. Tsang, X. Lu, S. K. So, B. S. Ong, *J. Mater. Chem. A*, **2017**, *5*, 23662-2367; b) L. Zhang, J. M. Cole, *J. Mater. Chem. A*, **2017**, *5*, 19541-19559.

[9] a) P. Roy, A. Jha, V. B. Yasarapudi, T. Ram, B. Puttaraju, S. Patil, J. Dasgupta, *Nature Communications* **2017***, 8*, 1716; b) G. E. Park, J. Shin, D. H. Lee, T. W. Lee, H. Shim, M. J. Cho, S. Pyo, D. H. Choi, *Macromolecules*, **2014**, *47*, 3747-3754.

[10] a) M. Chiu, B. H. Tchitchanov, D. Zimmerli, I. A. Sanhueza, F. Schoenebeck, N. Trapp, W. B. Schweizer, F. Diederich, *Angew. Chem. Int. Ed.* **2015**, *54*, 349-354; b) P. Gawel, C. Dengiz, A. D. Finke, N. Trapp, C. Boudon, J.-P. Gisselbrecht, F. Diederich, *Angew. Chem. Int. Ed.* **2014**, *53*, 4341-4345; c) A. D. Finke, O. Dumele, M. Zalibera, D. Confortin, P. Cias, G. Jayamurugan, J.-P. Gisselbrecht, C. Boudon, W. B. Schweizer, G. Gescheidt, F. Diederich, *J. Am. Chem. Soc.* **2012**, *134*, 18139−18146; d) S.-I. Kato, F. Diederich, *Chem. Commun.* **2010**, *46*, 1994-2006.

[11] a) M. Sekita, B. Ballesteros, F. Diederich, D. M. Guldi, G. Bottari, T. Torres, *Angew. Chem. Int. Ed.* **2016**, *55*, 5560-5564; b) T. Shoji, A. Maruyama, C. Yaku, N. Kamata, S. Ito, T. Okujima, K. Toyota, **2015**, 21, 402-409; c) G. Jayamurugan, A. D. Finke, J.-P. Gisselbrecht, C. Boudon, W. B. Schweizer, F. Diederich, *J. Org. Chem.* **2014**, *79*, 426-431; d) D. Koszelewski, A: Nowak-Król, D. T. Gryko, *Chem. Asian J.* **2012**, *7*, 1887-894; e) R. García, M. A. Herranz, M. R. Torres, P.-A. Bouit, J. L. Delgado, J. Calbo, P. M. Viruela, E. Ortí, N. Martín, *J. Org. Chem.* **2012**, *77*, 10707-10717; f) B. Breiten, Y.-L. Wu, P. D. Jarowski, J.-P. Gisselbrecht, C. Boudon, M. Griesser, C. Onitsch, G. Gescheidt, W. B. Schweizer, N. Langer, C. Lennartz, F. Diederich, *Chem. Sci.* **2011**, *2*, 88-93; g) A. Leliège, P. Blanchard, T. Rousseau, J. Roncali, *Org. Lett.* **2011**, *13*, 3098-3101.

[12] a) K. A. Winterfeld, G. Lavarda, J. Guilleme, M. Sekita, D. M. Guldi, T. Torres, G. Bottari, *J. Am. Chem. Soc.* **2017**, *139*, 5520-5529; b) M. Yamada, P. Rivera-Fuentes, W. B. Schweizer, F. Diederich, *Angew. Chem. Int. Ed.* **2010**, *49*, 3532-3535; c) M- Kivala, C. Boudon, J.-P. Gisselbrecht, B. Enko, P. Seiler, I. B. Müller, N. Langer, P. D. Jarowski, G: Gescheidt, F. Diederich, *Chem. Eur. J.* **2009**, *15*, 4111-4123; d) P. Reutenauer, M. Kivala, P. D. Jarowski, C. Boudon, J.-P. Gisselbrecht, M. Gross, F. Diederich, *Chem. Commun*. **2007**,*0*, 4898-4900.

[13] a) C. Romero-Nieto, R. García, M. A. Herranz, L. Rodríguez-Pérez, M. Sánchez-Navarro, J. Rojo, N. Martín, D. M. Guldi, *Angew. Chem. Int. Ed.* **2013**, 52, 10216-10220; b) J. Santos, E. M. Pérez, B. M.Illescas, N. Martín, *Chem. Asian J.* **2011**, *6*, 1848-1853.

[14] B. M. Illescas, N. Martín, *J. Org. Chem.* **2000**, *65*, 5986-5995.

[15] a) E. Ortí, R. Viruela, P. M. Viruela, *J. Phys. Chem.* **1996**, *100*, 6138-614; b) P. Bando, N. Martin, J. L. Segura, C. Seoane, E. Orti, P. M. Viruela, R. Viruela, A. Albert, F. H. Cano, *J. Org. Chem.* **1994**, *59*, 4618-4629.

[16] D. González-Rodríguez, T. Torres, D. M. Guldi, J. Rivera, M. A. Herranz, L. Echegoyen, *J. Am. Chem. Soc.* **2004**, *126*, 6301-6313.

[17] N. Martin, R. Behnisch, M. Hanack, *J. Org. Chem.* **1989**, *54*, 2563-2568.

[18] For UV-Vis studies of TCAQ-based D-A systems, see: a) F. Bures, O. Pytela, M. Kivala, F. Diederich, *J. Phys. Org. Chem.* **2011**, *24*, 274-281; b) F. Bures, O. Pytela, F. Diederich, *J. Phys. Org. Chem.* **2009**, *22*, 155-162; c) F. Bureš, W. B. Schweizer, C. Boudon, J.-P. Gisselbrecht, M. Gross, F. Diederich, *Eur. J. Org. Chem.* **2008**, 994-1004; d) B. Illescas, N. Martin, J. L. Segura, C. Seoane, E. Orti, P. M. Viruela, R. Viruela, *J. Org. Chem.* **1995**, *60*, 5643–5650.

[19] a) S.-i. Kato, M. Kivala, W. B. Schweizer, C. Boudon, J.-P. Gisselbrecht, F. Diederich, *Chem. Eur. J.* **2009**, *15*, 8687-8691; b) T. Michinobu, C. Boudon, J.-P. Gisselbrecht, P. Seiler, B. Frank, N. N. P. Moonen, M. Gross, F. Diederich, *Chem. Eur. J.* **2006**, *12*, 1889-1905.

[20] M. J. Frisch, G. W. Trucks, H. B. Schlegel, G. E. Scuseria, M. A. Robb, J. R. Cheeseman, G. Scalmani, V. Barone, B. Mennucci, G. A. Petersson, H. Nakatsuji, M. Caricato, X. Li, H. P. Hratchian, A. F. Izmaylov, J. Bloino, G. Zheng, J. L. Sonnenberg, M. Hada, M. Ehara, K. Toyota, R. Fukuda, J. Hasegawa, M. Ishida, T. Nakajima, Y. Honda, O. Kitao, H. Nakai, T. Vreven, J. A. Montgomery, J. E. Peralta, F. Ogliaro, M. Bearpark, J. J. Heyd, E. Brothers, K. N. Kudin, V. N. Staroverov, R. Kobayashi, J. Normand, K. Raghavachari, A. Rendell, J. C. Burant, S. S. Iyengar, J. Tomasi, M. Cossi, N. Rega, J. M. Millam, M. Klene, J. E. Knox, J. B. Cross, V. Bakken, C. Adamo, J. Jaramillo, R. Gomperts, R. E. Stratmann, O. Yazyev, A. J. Austin, R. Cammi, C. Pomelli, J. W. Ochterski, R. L. Martin, K. Morokuma, V. G. Zakrzewski, G. A. Voth, P. Salvador, J. J. Dannenberg, S. Dapprich, A. D. Daniels, O. Farkas, J. B. Foresman, J. V. Ortiz, J. Cioslowski, D. J. Fox, *Gaussian 09, Revision D.01*, Wallingford CT, 2009.

[21] a) A. D. Becke, *J. Chem. Phys.* **1993,** *98*, 5648-5652; b) C. Lee, W. Yang, R. G. Parr, *Phys. Rev. B* **1988,** *37*, 785-789.

[22] M. M. Francl, W. J. Pietro, W. J. Hehre, J. S. Binkley, M. S. Gordon, D. J. Defrees, J. A. Pople, *J. Chem. Phys.* **1982,** *77*, 3654-3665.

[23] G. A. Zhurko, ChemCraft 1.8. http://www.chemcraftprog.com

[24] a) M. E. Casida, C. Jamorski, K. C. Casida, D. R. Salahub, *J. Chem. Phys.* **1998,** *108*, 4439-4449; b) C. Jamorski, M. E. Casida, D. R. Salahub, *J. Chem. Phys.* **1996,** *104*, 5134-5147; c) M. Petersilka, U. J. Gossmann, E. K. U. Gross, *Phys. Rev. Lett.* **1996,** *76*, 1212-1215.

[25] Y. Zhao, D. G. Truhlar, *J. Phys. Chem. A* **2004,** *108*, 6908-6918.

[26] G. Scalmani, M. J. Frisch, *J. Chem. Phys.* **2010,** *132*, 114110.

FULL PAPER

**Twisting conjugation:** Cycloaddition-retroelectrocyclization reactions between tetracyanoethylene and push-pull chromophores based on 11,11,12,12-tetracyano-9,10-anthraquinodimethane (TCAQ) and one or two dimethylaniline (DMA) units provide new chromophores with significant electronic communication despite the largely bent geometry adopted by the formed 1,1,4,4-tetracyanobuta-1,3-diene (TCBD) units

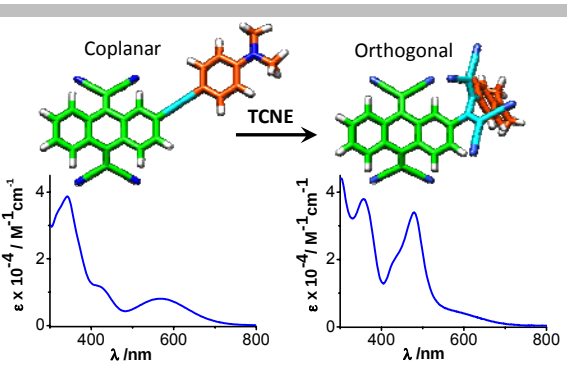


*Raúl García, Joaquín Calbo, Rafael Viruela, Mª Ángeles Herranz,* Enrique Ortí* and Nazario Martín**

**Planarity vs. Non-Planarity in the Electronic Communication of TCAQ-Based Push-Pull Chromophores**